ELSEVIER

Biochimica et Biophysica Acta 1230 (1995) 10–22

BBA Biochimica et Biophysica Acta

Further characterization of the chloroplast grana margins: the non-detergent preparation of granal Photosystem I cannot reduce ferredoxin in the absence of $NADP^+$ reduction

Louie Wollenberger [a], Claes Weibull [b], Per-Åke Albertsson [a,*]

[a] *Department of Biochemistry, University of Lund, P.O. Box 124, S-221 00 Lund, Sweden*
[b] *Department of Microbiology, University of Lund, P.O. Box 124, S-221 00 Lund, Sweden*

Received 4 November 1994; revised 20 January 1995; accepted 30 January 1995

Abstract

The chloroplast grana margins of spinach thylakoids were isolated by sonication and aqueous-two-phase partitioning and their electron transport properties examined. Photosystem II and I electron transport activities were measured and compared to the appressed and non-appressed grana core and stroma lamellae, respectively, as well as to whole thylakoids. The results show that the PS II complexes in the grana margins are of the PS II_β subtype with respect to antenna size, but are Q_B reducing with respect to the acceptor side properties, while the PS I centers in the grana margins have slightly larger antennae as compared to the PS I centers in the stroma lamellae and are more like the PS I_α centers located in the grana domain. The ability to reduce ferredoxin and $NADP^+$ was also tested and it was found that the grana margin membrane fraction was unable to reduce ferredoxin, even in the presence of added artificial electron donors. The stroma lamellae and whole thylakoid fractions both reduced ferredoxin at high rates. However, the grana margins could catalyze the reduction of $NADP^+$ when supplied with the necessary components (ferredoxin, ferredoxin:$NADP^+$ oxidoreductase, and an electron source). The results suggest that the PS I populations located in the margins of the grana domain are functionally different from the PS I centers located in the stroma lamellae. The data support a model whereby the PS I centers in the grana are primarily involved in non-cyclic electron transport, while the PS I centers located in the stroma lamellae are capable of participating in both cyclic and non-cyclic electron transport.

Keywords: Chloroplast; Grana margin; Light harvesting complex II; Photosystem; Partitioning; Aqueous polymer; Ferredoxin:NADP oxidoreductase; (Spinach thylakoid)

1. Introduction

Recently, we described the properties of a unique sub-chloroplast membrane fraction obtained by sonicating the grana or so called 'inside-out' vesicle fraction of spinach chloroplast thylakoids and then separating the membrane fragments by means of liquid-liquid aqueous polymer two-phase partitioning [1], a procedure in which a heterogeneous mixture of biological membranes can be fractionated into homogeneous populations if their surface associated properties are significantly dissimilar [2–4]. Strikingly, it was found that the ultrasonic fragmentation of inside-out grana vesicles specifically, and reproducibly, removed a population of membrane vesicles enriched in Photosystem I and poor in Photosystem II relative to the granal material remaining after the sonication and separation procedure [1,5]. The new PS-I-rich sub-granal membrane fraction partitioned to the top phase of an aqueous two-phase system, while the remaining PS-II-rich inside-out vesicles, representing the central region of the grana, partitioned to the interface. In this way, and following

Abbreviations: chl, chlorophyll; PS II, Photosystem II; PS I, Photosystem I; LHCII, light harvesting complex II; P700, the primary electron donor of PS I; DMSO, dimethyl sulfoxide; $NADP^+$, nicotinamide adenine dinucleotide phosphate (oxidized form); FNR, ferredoxin:$NADP^+$ oxidoreductase; SDS, sodium dodecyl sulfate; DCIP, 2,6-dichlorophenol-indophenol; DBMIB, 2,5-dibromo-3-methyl-6-isopropyl-*p*-benzoquinone; PpBQ, phenyl-*p*-benzoquinone; DQ, duroquinone, tetramethyl-*p*-benzoquinone; PQ, plastoquinone; PEG, poly(ethylene glycol); KCN, potassium cyanide; MV, Methyl viologen; *P*, partition ratio for cells or particulates defined as the quantity in a bulk phase as a percentage of the total cells added.

* Corresponding author. Fax: +46 46 104534.

SSDI 0005-2728(95)00027-5

three to four extraction steps, each of the sub-granal membrane fractions could be isolated in pure form and their photochemistry could be studied.

The preliminary report demonstrated that the PS-I-rich portion of the grana possessed a unique protein composition when compared to both the appressed and non-appressed domains. In particular, it was found that this new membrane material was enriched in the 64 kDa protein, claimed to be a kinase, and that it was slightly depleted in cytochrome *f* [1]. Furthermore, the surfeit of chlorophyll *b* in the margin fraction which could not be assigned to PS II when fluorescence induction kinetics were measured was tentatively assigned to the PS I complex on the basis of a faster rate of photooxidation for P700 as compared to the PS I found in the stroma lamellae [1]. This was supported by an earlier report from this laboratory where it was shown, using low-temperature fluorescence and P700 photoxidation kinetics, that the majority of the LHCII located in the chloroplast grana margins was functionally coupled to PS I and that this 'special' pool of LHCII had a different oligomeric composition as compared to the central core of the grana [6]. Considering all the evidence detailed in the first report [1], and all other previously published reports by others covering fractionation and immunogold labeling of chloroplast thylakoids [7–13], we reasoned that the sonication of 'intact' grana vesicles was an effective, non-detergent method for removing the peripheral portions of the membranes which, in the unfragmented, stacked chloroplast thylakoid represented the highly curved and non-appressed margins of the grana stacks, areas known to contain PS I, ATPase and ferredoxin-NADP reductase [7–10].

It appeared that we had isolated the granal population of PS I whose close association with PS II located in the partitions of the grana has, in the past, led us and others to conclude that these marginal PS I centers play a different role in photchemical electron transport as compared to the stromal lamellae PS I centers located farther away [14–16]. In fact, these interpretations were not new, but had first been alluded to in the pioneering fragmentation studies carried out by Jacobi and Lehmann, Sane et al., and Arntzen et al. in the late 1960's and early 70's, when the presence of a granal population of PS I first received attention [11–13].

The fact that the margin vesicles are in a right-side-out orientation following sonication of the 'intact' inside-out grana vesicles [1,5] and that they are enriched in granal PS I makes them an excellent starting material for comparison studies with the right-side-out stroma lamellae vesicles as well as for investigations into the effects that environmental stress factors have on the domain organization of the electron transport system within the thylakoid membrane.

In this report, using an improved preparation procedure with greater yield, we examine in detail the electron transport properties of the PS II and PS I populations located in the grana margins.

2. Materials and methods

2.1. Chemicals

Ferredoxin and ferredoxin:$NADP^+$ oxidoreductase from spinach (EC 1.18.1.2) and $NADP^+$ were all purchased from Sigma Chemical Co (St. Louis, MO, USA). The antibody to ferredoxin:NADP oxidoreductase from barley was donated by Birger Lindberg Møller of the Plant Biochemistry Laboratory, Royal Veterinary and Agricultural University, Copenhagen, Denmark.

2.2. Preparation of chloroplast thylakoids and sub-thylakoid membrane fractions

Spinach (*Spinacia oleracia L. medania*) was grown at 20° C with a light period of 12 h and intensity of 400 $\mu E\, m^{-2}\, s^{-1}$ and was cut and dark-adapted at 4° C for 3 days prior to homogenization. Thylakoid membranes were prepared and fractionated into grana (B3) and stroma lamellae (T3) vesicle populations using a combination of sonication and aqueous polymer (dextran-poly(ethylene glycol)) two-phase partitioning as described in [17] except that four partitioning steps were carried out instead of just three to further ensure complete separation of the grana and stroma lamellae compartments (Fig. 1). The grana margins were isolated by sonicating the grana (B4), also called the inside-out vesicle, population followed by two-phase partitioning as is described in detail in [1] except that instead of sonicating the grana for 6×30 s we sonicated for 12×30 s and the sonicated grana was extracted twice with fresh top phase, as illustrated in Fig. 2, instead of just once as in [1]. The sonication of the thylakoid and sub-thylakoid membrane material takes place directly in the aqueous polymer two-phase system at 0° C. Partitioning occurs at 4° C. Membrane fractions were washed free of the polymers by dilution in 100 mM sucrose/10 mM sodium phosphate buffer (pH 7.4)/5 mM NaCl and high-speed centrifugation. The samples were then resuspended in a small volume of the same buffer +5% DMSO and stored in liquid nitrogen. The properties and character of these membrane vesicle fractions have all been described previously [1,5,18,19].

2.3. Analysis

Total protein was assayed according to Beardon [20] using Triton X-100 to solubilize the membrane protein [21]. The concentration of P700 was determined from the light minus dark absorbance change at 700 nm using an Aminco DW-2 spectrophotometer operating in the split-beam mode [22]. The reaction buffer contained 0.02% SDS (w/v)/2 mM methylviologen, 2 mM ascorbic acid, 15 mM Tricine (pH 7.8), 5 mM $MgCl_2$, 10 mM NaCl, 400 mM sucrose, and sample for a final chlorophyll concentration of 20 to 30 μM.

Chlorophyll concentrations were measured according to Arnon [23] and also according to Lichtenthaler [24]. Total carotenoid content was measured using the equations of Lichtenthaler [24]. The solvent for all cases was 80% acetone (v/v).

Absorption spectroscopy at 77 K was measured on a Shimadzu UV-3000 spectrophotometer equipped with a low-temperature attachment. The sample was diluted to 50 μg Chl/ml with a buffer comprised of 50 mM Tricine (pH 7.8)/400 mM sucrose/10 mM NaCl/5 mM $MgCl_2$/66% glycerol (v/v). The pathlength of the cuvette was 1 mm.

Fluorescence emission spectra at 77 K were recorded with a Spex Fluorolog 2 spectrofluorometer with double monochronomators and a cooled RCA C31034 photomultiplier operated in the photon-counting mode. The same buffer as for low-temperature absorption spectroscopy (see above) was used. The sample concentration was 10 μg Chl/ml. The excitation wavelength was 472 nm. The excitation and emission slit widths were set at 2 and 1 nm, respectively.

2.4. Electron microscopy

Samples for electron microscopy were fixed overnight at 4° C with 1% osmium tetroxide, dehydrated with acetone and embedded in epoxy resin (Agar 100, Agar Scientific, UK). Thin sections were stained with 5% uranyl acetate at room temperature for 45 min and examined with a Philips EM 300 electron microscope working at 60 kV.

2.5. Electron transport measurments

PS I and PS II activities were measured using a Clark-type O_2 electrode (Hansatech, Norfolk, UK). The actinic light was provided by a slide projector and was transmitted through an interference filter to give red light spanning 600 to 700 nm. In the case of PS I, electron transport from reduced DCIP to Methyl viologen was measured and the buffer comprised 100 mM sucrose, 50 mM Tricine (pH 7.9), 10 mM NaCl, 5 mM $MgCl_2$ and 3 mM K_2HPO_4. The final volume for each assay was 1 ml and included 3 mM NH_4Cl/500 μM NaN_3/300 μM DCIP/10 mM ascorbic acid/120 μM Methyl viologen/20 μM DCMU and 25 μg chlorophyll of the membrane sample.

For PS II measurements, electron transport from H_2O to PpBQ (300 mM) was measured and the buffer consisted of 100 mM sucrose/50 mM Mes (pH 6.5)/10 mM NaCl/5 mM $MgCl_2$. The sample concentration was 20 to 25 μg Chl/ml (1 ml final volume). Other assays comparing the reduction potential of PS II were done using either duroquinone or phenyl-*p*-benzoquinone at a concentration of 200 μm in both cases. All electron transport measurments were made at 20° C.

To inhibit plastocyanin, membrane fractions were first thawed and dark adapted on ice for 20 to 30 min, then diluted to 0.5 μg Chl/ml in the same buffer used for PS I electron transport (described above) containing in addition 0.15 M KCN and then incubated in the dark for 2 h at 0° C. Aliquots (50 μl) equal to 25 μg Chl were removed and the PS I activity measured directly in a final volume of 1 ml as described above.

2.6. Measurement of feredoxin and $NADP^+$ reduction

The reduction of ferredoxin by uncoupled (NH_4Cl) membrane fractions was followed spectrophotometrically at 463 nm at room temperature according to Cleland and Bendall [25] in an Aminco DW-2 spectrophotometer except that only 2 μM ferredoxin was used and DCIP and ascorbic acid could be included at 130 μM and 4.5 mM, respectively. An absorbance coefficient of 8.97 $mM^{-1}\,cm^{-1}$ for Fd_{ox} was used [25]. Prior to the measurements, the buffer, comprised of 100 mM sucrose/50 mM Tricine (pH 7.9)/5 mM $MgCl_2$/5 mM KH_2PO_4/6 mM glucose, was flushed with nitrogen gas. Glucose oxidase and catalase were included in the assay mixture to maintain anaerobicity [25]. The concentration of the sample was 11 ug/ml. Where indicated, $NADP^+$ was added to 2 mM. The sample cuvette was illuminated from the side with saturating red light. A 455 nm interference filter (half-bandwidth 50 nm) and a cut-off 600 nm filter were placed in front of the photomultiplier.

The assay for $NADP^+$ reduction was carried out just as for ferredoxin reduction except that the absorbance change was followed at 340 nm and a 340 nm interference filter was placed in front of the photomultiplier. The buffer, assay mixture and chlorophyll concentration were exactly the same as for the measurement of ferredoxin reduction. In some cases, 0.3 U/ml ferredoxin-NADP reductase was included; these are indicated clearly in the respective figures (Results section). An absorbance coefficient of 5.1 $mM^{-1}\,cm^{-1}$ for NADH at 340 nm was used [26].

2.7. Western blotting

The membrane-bound protein was first fractionated by SDS-PAGE using the buffer system of Laemmli [27] in the presence of 4 M urea with an acrylamide gradient from 12 to 22.5%. The protein was then electrophoretically transferred from the polyacrylamide gel to a poly(vinylidene difluoride) membrane (PVDF, Immobilon™, Millipore) using a Kem En Tec semi-dry blotting apparatus (UKA Biotech Denmark). The immuno-detection of the blotted protein was then carried out using a Bio-Rad Immuno-blot assay kit. The secondary antibody was conjugated to alkaline phosphatase.

3. Results

3.1. Preparation of the grana margins

Preparation of the grana margins proceeds in two fragmentation steps as illustrated in the flow chart in Fig. 1.

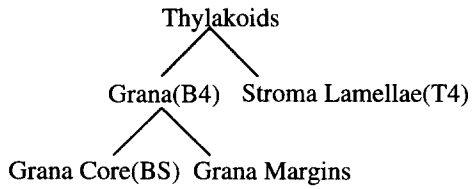

Fig. 1. A flow chart showing the relationships and derivations of the three sub-thylakoid membrane fractions representing the core and margins of the appressed membrane domain and the non-appressed stroma lamellae obtained by the sonication and separation procedure [15]. The composition of the two-phase system was the same as given in the caption to Fig. 2.

First, a breakage of thylakoids to yield the stroma lamellae and grana compartments followed by a final sonication step applied to the grana population to yield the margins and core of the appressed region [1,5]. Each round of sonication is followed by four partitioning or extraction steps and the two-phase system employed for the extractions is designed such that inside-out membranes enriched in PS II-LHCII have a lower partition ratio, P, and partition to the interface and bottom phase, while right-side-out membranes enriched in PS I and ATPase have a higher P and partition to the top phase (see [2,3,17] for a discussion about aqueous two-phase partitioning in general and see [17] for a discussion of the method as applied to chloroplast thylakoid fragments) giving rise to the nomenclature: B4 (bottom phase, four extractions) and T4 (top phase, four extractions) (Fig. 1).

Fig. 2 depicts in detail the extraction procedure carried out to prepare the grana margins following sonication of grana vesicles, a technique often referred to as the 'batch' procedure of preparation. This method for preparation of the grana margins differs in two major respects from the version published in our first report [1]. Here, we have doubled the number of sonication pulses delivered to the grana vesicles and secondly, following sonication, the fragmented grana vesicles are extracted twice (instead of just once as before [1]) with fresh top phases which are themselves each extracted twice with fresh bottom phases, to remove contaminating inside-out vesicles, and then pooled together to comprise the final margin population as shown in Fig. 2. These modifications increase the yield of the margins by a factor of 4 as compared to the earlier procedure (Table 1).

Fig. 3 shows electron microscopic images taken of thin sections of the grana core and grana margins vesicle preparations. The margin vesicles are round shaped with

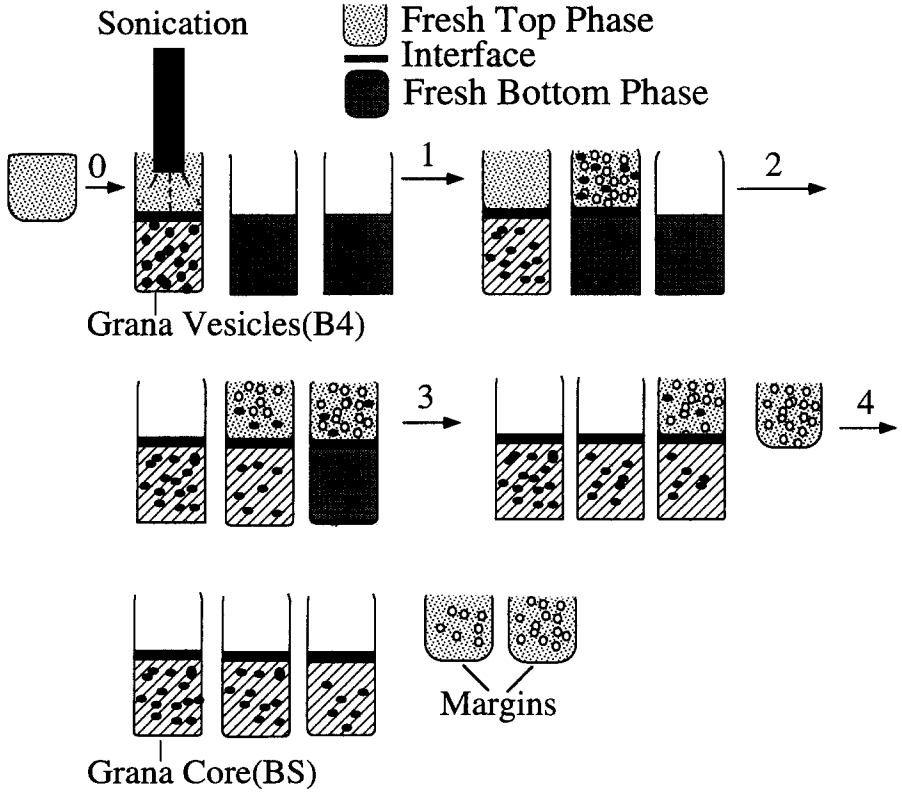

Fig. 2. A schematic illustration of the sonication and separation procedure used to prepare the grana margins and core membrane fractions of spinach thylakoids. Inside-out grana vesicles suspended in an aqueous polymer two-phase system are sonicated 12 × 30 s with 1 min resting intervals and under continuous cooling (0° C). Following sonication, the two-phase system is equilibrated to 4° C, mixed, and centrifuged to separate the phases. The newly formed PS-I-rich grana fragments (the margins) partition to the PEG rich top phase, while the PS-II-rich grana core prefers the dextran rich bottom phase. The phase system comprised 5.8% (w/w) dextran/5.8% (w/w) poly(ethylene glycol)/20 mM sucrose/10 mM sodium phosphate buffer (pH 7.4)/5 mM NaCl.

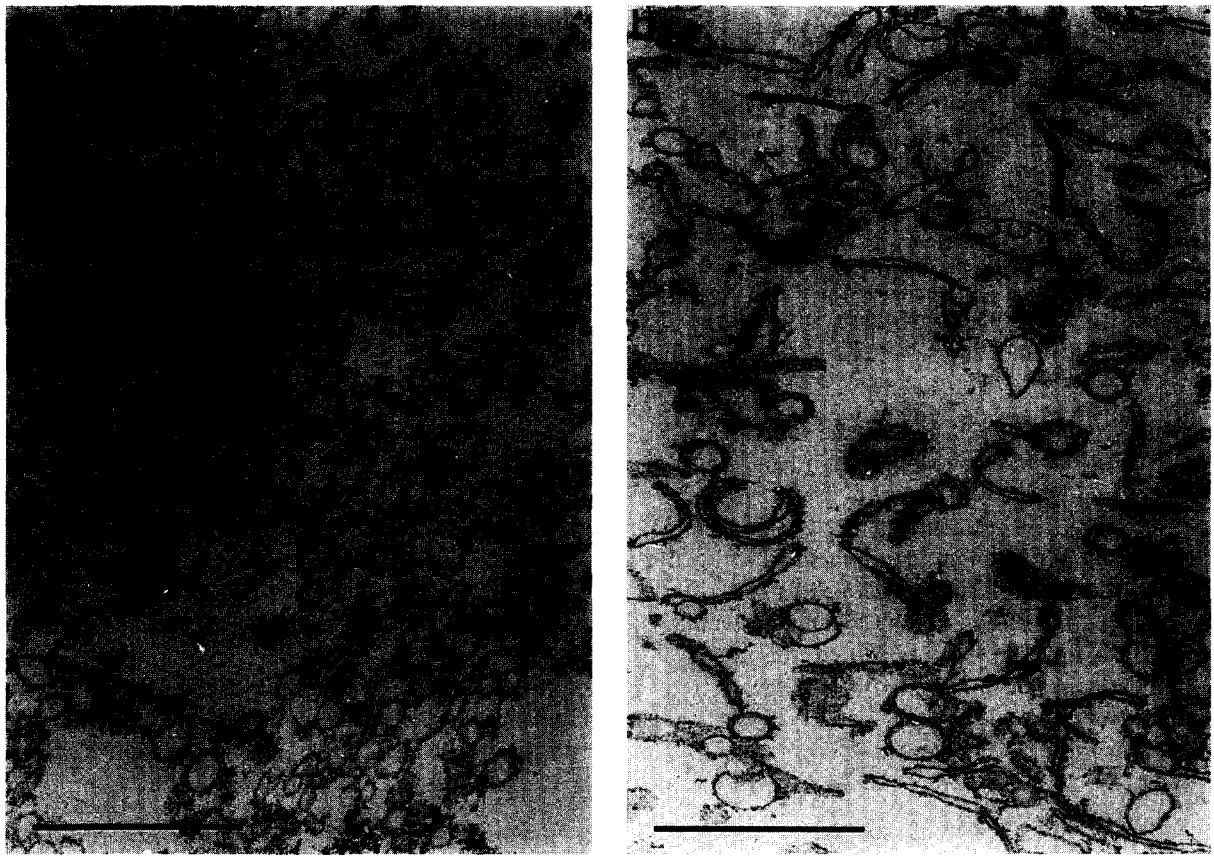

Fig. 3. Electron microscopy of thin sections of the grana margins (a) and grana core (b) membrane preparations. The bar represents 1 μm.

an average diameter of around 150 nm. The grana core vesicles are flattened sheets with a diameter of about 500 nm. If these vesicles reflect the size of the actual domains in the thylakoid, the grana margins comprise roughly 20 to 25% of the surface area of the grana stacks for spinach grown under these conditions (see Materials and methods). The yield of each fraction, in terms of total chlorophyll, also support this conclusion (Table 1).

3.2. Pigment-protein composition

Three membrane fractions, representing the three primary structural domains of the thylakoid, are obtained by the sonication and separation procedure. Table 1 summarizes the properties of these fractions in terms of the PS I, light absorbing pigment, and total protein contents (Table 1). Prior to fragmentation grana vesicles (B3) contain between 1.5 and 1.4 mmol/mol P700/Chl [19]. Sonication removes the PS-I-rich portion of the grana vesicles, the margins (2.45 mmol/mol P700/Chl), leaving an even more PS-I-depleted grana core particle (1.19 mmol/mol P700/Chl) (Table 1). The stroma lamellae contains the most protein per chlorophyll as compared to all other membrane fractions due to the enrichment of the ATPase complex in the non-appressed areas, while the grana core is more enriched in the chlorophyll *a/b* binding proteins of LHCII associated with PS II. This is borne out by the chlorophyll *a/b* ratios, which range from above 5 for the stroma lamellae down to nearly 2 g/g for the central area of the appressed region. The corresponding values ob-

Table 1
A summary of the pigment and total protein contents of the various thylakoid membrane fractions

Membrane fraction	Chlorophyll				P700		Protein
	yield%	*a/b* [a] (g/g)	*a/b* [b] (g/g)	Chl/Car [b] (g/g)	yield%	P700/Chl (mmol/mol)	protein/Chl (g/g)
Thylakoids	100	3.01	3.21	4.55	100	2.64	2.84
Grana core	12	2.24	2.33	4.25	5	1.19	2.25
Grana margins	4	2.96	3.14	4.35	4	2.45	2.80
Stroma lamellae	11	4.96	5.57	4.43	18	4.30	3.67

[a] Chlorophyll determined according to Arnon [23].
[b] Chlorophyll and total carotenoids determined according to Lichtenthaler [24].

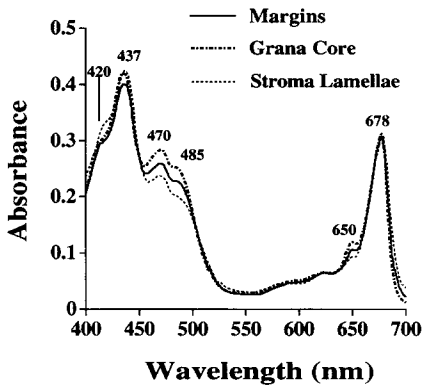

Fig. 4. Low-temperature absorbance (77 K) of the three sub-thylakoid membrane fractions.

tained for the grana margins fall between those of the grana core and stroma lamellae and describe an area of the membrane whose boundries may cross into both the appressed and non-appressed domains.

Interestingly, despite large variations in chlorophyll *a/b* composition, and irrespective of the heterogeneous distribution of the two photosystems between the appressed and non-appressed domains, the total carotenoid content per total chlorophyll is relatively constant throughout the thylakoid membrane, about 4 to 4.5 g Chl/g Car. These values translate to roughly 2.9 to 2.7 mol Chl/mol Car for the thylakoid and grana core fractions, respectively [28].

3.3. Low-temperature absorption and fluorescence emission spectra

Low-temperature absorption spectra for each of the three membrane domains are shown in Fig. 4. At 77 K the absorption maxima at 650 and 470 nm belonging to chlorophyll *b* are enhanced and the overlayed spectra clearly illustrate the quantitative differences in LHCII content for each of the domains (Fig. 4). The light-harvesting antennae complexes of PS II are also enriched for the xanophylls lutein and neoxanthin [24,28,29], which are expected to augment the absorption in the area 450 to 500 nm. The stroma lamellae spectrum contained, in addition, a slight shoulder at 420 nm probably due to chlorophyll *a* (Fig. 4).

Fluorescence emission spectra at 77 K were also recorded for the sub-chloroplast membrane fractions (Fig. 5). At this temperature, the spectra are characterized by three major peaks: two at 685 and 695 nm belonging to PS II, and a third at 735 nm where PS I makes a large contribution [30]. Since these peak assignments are not absolute it is not possible or correct to make accurate quantitative assessments of PS II and PS I contents of the membrane fractions based soley on fluorescence emission amplitudes. However, the spectra are useful in a qualitative manner for estimating and comparing the relative amounts of PS-II- and PS-I-associated chlorophyll species present in each of the thylakoid membrane domains.

The two photocenters appear to be most evenly intermixed in the grana margins. About twice as much PS II per total chlorophyll is present in the grana margins as in the stroma lamellae (Fig. 5). These estimates are supported by electron transport activity measurements as discussed below.

3.4. PS I and PS II electron transport activities

Both PS II and PS I are heterogeneous with regard to antenna size [19,31,32]. This is especially evident when the thylakoid membrane is fragmented and the grana and stroma lamellae domains are studied separately [19,32]. PS II_α and PS I_α, which have the largest antennae, are located in the grana of the thylakoid membrane, while PS II_β and PS I_β have the smallest antennae and are located in the stroma lamellae [19,31,32]. It was important to determine the character of PS II and PS I in the grana margins and compare them with the corresponding populations in the grana partitions and stroma lamellae. Therefore, the light-saturation kinetics of PS I and PS II activity were measured for each of the membrane fractions and the data plotted to determine the maximum velocity (V_{max}) and to estimate the relative antenna size (K_M) for each photosystem [19]. These data are shown in Figs. 6 and 7 for PS I

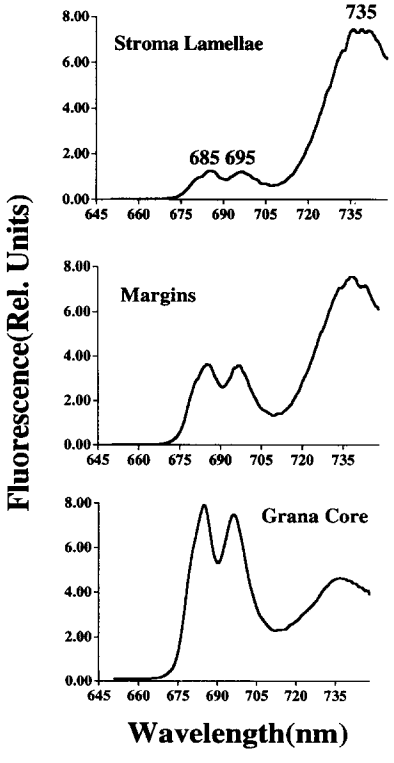

Fig. 5. Low-temperature fluorescence (77 K) emission spectra of the stroma lamellae (top), grana margins (middle) and grana core (bottom) membrane fractions.

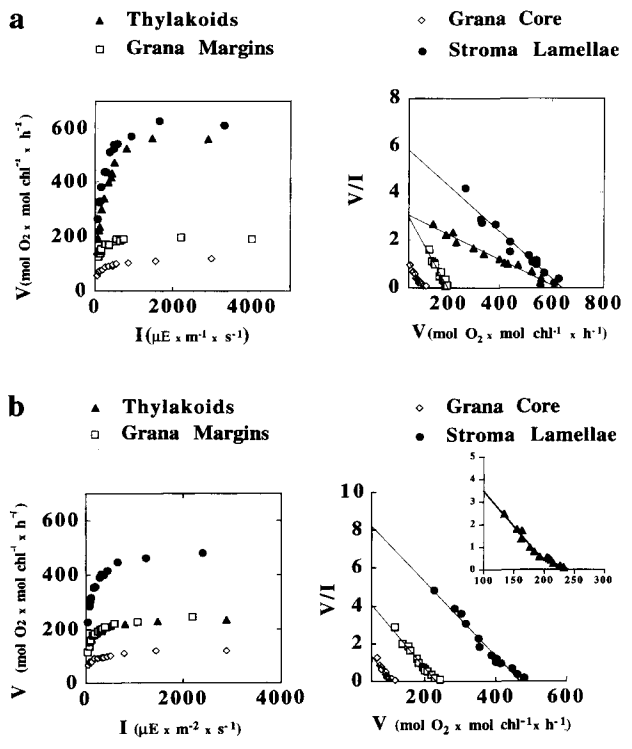

Fig. 6. (a) The rates of Photosystem I catalyzed electron transport of thylakoid and sub-thylakoid membrane fractions when plotted first as an asymptotic function of light intensity (left) and second as a straight line, V/I vs. V (right) for which the slope is equal to $-1/K_M$ and the x-intercept is equal to V_{max}. (b) The same as for (a) except following incubation in KCN. The straight line plot of thylakoids is shown separately in the upper right to illustrate how the data deviate from linearity, suggesting the existence of some heterogeneity in the total pool of PS I.

and PS II, respectively. In addition, the PS I activities for each case were measured before and after the inhibition of plastocyanin by KCN (Fig. 6a and 6b, respectively). The plot in the left portion of each the figures shows the saturation of the activities with increasing light intensity, while the the plot on the right shows the same data fitted to a straight line using the Eadie-Hofstee formulation of Michaelis-Menten kinetics [33,34]; the slopes are equal to $-1/K_M$. The kinetic constants for each of the membrane samples are given in Table 2. The K_M, and consequently the antenna size, of the PS I in the grana margins most resembles the PS I in the grana core, PS I_α, but the antennae of the PS II located in the grana margins are closest in size to the PS II_β centers located in the stroma lamellae.

The data obtained for the KCN poisoned membrane fractions demonstrate that the grana margins contain no residual plastocyanin and that they must therefore derive from the same inside-out membrane fraction that the grana core fraction derives from (Fig. 6b, Table 2). No decrease in the PS I activities of either the grana margins or the grana core fractions are observed following incubation in KCN, while the stroma lamellae and whole thylakoid fractions lost 26% and 63% of their activities, respectively. It is known that right-side-out vesicles from the stroma lamellae retain about 25% of the original plastocyanin following fragmentation of the thylakoid [35]. Note as well that the PS I activities of the thylakoid and grana margins fractions are the same after KCN treatment, something we would expect, since both fractions have about the same P700/Chl (Table 1), and means conversely that the turnover rates of the granal PS I centers are probably 2–3-times faster in vivo when they are saturated with plastocyaninthan we can measure here in vitro. Following KCN treatment, differences in antennae sizes for PS I are harder to distinguish with this technique, though some curvature in the straight line plot of whole thylakoids is apparent (Fig. 6b), suggesting that some heterogeneity still exists in the PS I population. However, a difference in antenna size between KCN-treated fractions from the stroma lamellae and grana core has been demonstrated before using P700 photo-oxidation kinetics [19,32].

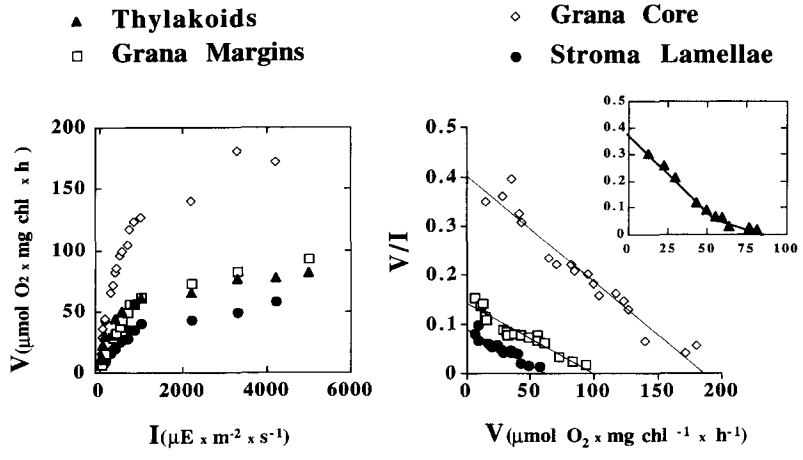

Fig. 7. The rates of Photosystem-II-catalyzed electron transport of thylakoid and sub-thylakoid membrane fractions as a function of light intensity (left) and when plotted according to the straight line formula of Eadie and Hofstee, V/I vs. V (right). The V/I vs. V plot of whole thylakoids is shown separately (upper right) to indicate how the heterogeneity of the PS II population is revealed by the curvature of the straight line plot.

3.5. Acceptor side properties of PS II

In addition to differences in antenna size, the PS II_α and PS II_β reaction centers have been shown to have different redox potentials [36–38]. Henrysson and Sundby demonstrated that whole chain electron transport is deficient in stroma lamellae vesicles due to the inability of PS II_β to reduce endogenous plastoquinone (non-Q_B reducing) [39], which has a midpoint potential value that is slightly more negative than that of PS II_β [37,40]. Two of the artificial electron acceptors used in that study, duroquinone and phenyl-*p*-benzoquinone, have similar lipophilicities but differ greatly with respect to midpoint potential, making them ideal candidates for comparing the redox properties of different PS II populations regardless of their orientation in the membrane. Table 3 compares the curtailment in oxygen evolving activity for the three sub-thylakoid membrane fractions when duroquinone was substituted for phenyl-*p*-benzoquinone as the acceptor of electrons from PS II. The largest drop in PS II activity was observed for the stroma lamellae fraction, for which the activity decreased by 74%. The grana core and grana margins lost just 18 and 32% of their O_2-evolving capacity, respectively, suggesting that the majority of the PS II centers in the grana margins are of the Q_B reducing variety [37,41].

3.6. Reduction of ferredoxin and $NADP^+$

The light-induced absorbance changes occurring at 463 and 340 nm were followed to measure the reduction of ferredoxin [25] and $NADP^+$ respectively by the thylakoid membrane fractions. As a pilot experiment, we compared the fractions in a purely qualitative manner for their abilities to catalyze the reduction of ferredoxin. Only the thylakoid and stroma lamellae membrane fractions could reduce ferredoxin to any significant extent (Fig. 8). Re-

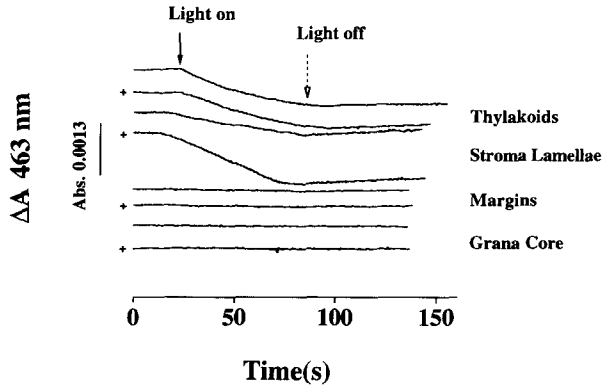

Fig. 8. The light-induced reduction of ferredoxin by thylakoid and sub-thylakoid membrane fractions. Upon reduction by Photosystem I, the absorbance of ferredoxin at 463 nm decreases. Each fraction was measured twice, first in the absence of any artificial electron donors, and second in the presence of ascorbate and DCIP(+). These measurements were made qualitatively to compare the relative absorbance changes taking place for each fraction and shows in a clear manner the inability of the PS I in the grana margins and grana core to reduce ferredoxin, whereas the PS I in both the stroma lamellae and intact thylakoid membranes are able to catlayze the reduction of ferredoxin. The presence of ascorbate and DCIP does not seem to enhance the rate or degree of the absorbance change in the case of whole thylakoids, but greatly enhances the reduction in the case of the stroma lamellae.

Table 2
A summary of the kinetic constants K_M and V_{max} for the PS I and PS II populations located in the stroma lamellae, grana margins, and grana core, and compared to unfragmented thylakoids

Membrane fraction	PS I activity						PS II activity	
	control			KCN-treated				
	K_M	V_{max}	V_{max}/P700	K_M	V_{max}	V_{max}/P700	K_M	V_{max}
Thylakoids	189	625	237		232	88		82
Stroma lamellae	102	642	149	53	473	110	714	63
Grana margins	50	201	82	45	234	96	714	101
Grana core	49	105	88	47	113	95	476	191

Activities for PS I are given in mol O_2/mol Chl per h, and for PS II in μmol O_2/mg Chl per h. A turnover number (V_{max}/P700) could be computed for PS I but not for PS II, since the absolute concentration of PS II was not measured.

Table 3
The rates of oxygen evolution (μmol O_2/mg Chl per h) by the Photosystem II centers in the thylakoid and sub-thylakoid membrane fractions when measured in the presence of either PpBQ or DQ

Electron acceptor	Acceptor side properties of PS II				
	E_m (mV)	grana core	grana margins	stroma lamellae	thylakoids
Phenyl-*p*-benzoquinone	279	212	124	51	98
Duroquinone	52	173	84	13	43
% decrease in activity		18%	32%	74%	56%

The redox potentials of the quinones were taken from Ref. [40]. Only those PS II centers with reduction potentials below that of the quinone oxidant will contribute significantly to the rate of oxygen evolution.

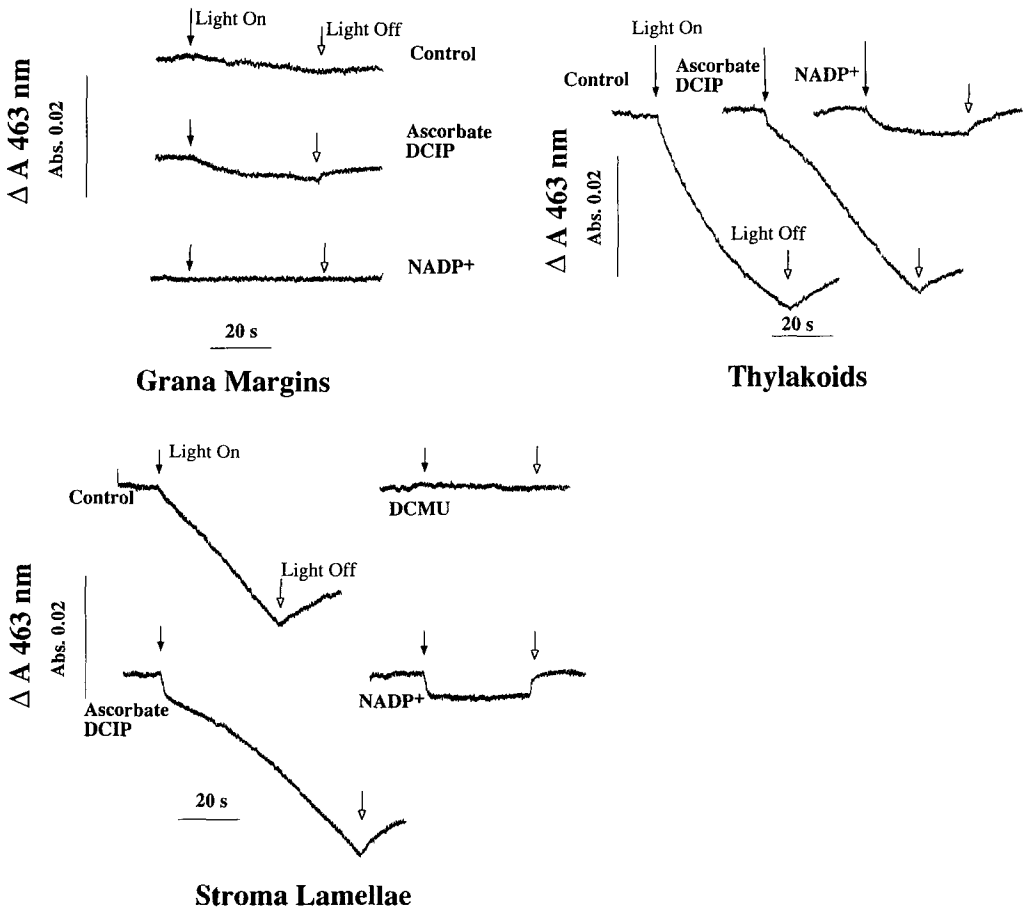

Fig. 9. The reduction of ferredoxin by the right-side-out, PS-I-rich thylakoid membrane fractions. For each membrane fraction, the assay was conducted in sequence on the same reaction mixture (absorbance traces from left to right in the case of thylakoids, or from left to right top to bottom in the case of the stroma lamellae, and from top to bottom in the case of the grana margins) measuring first in the absence of any artificial electron donors (control), following the addition of ascorbate and DCIP, and lastly following the addition of $NADP^+$. In the case of the stroma lamellae, an extra measurement was made in the presence of DCMU. Note that the stroma lamellae are able to carry out whole chain electron transport (control). $NADP^+$ prevents the absorbance changes from taking place, probably by oxidizing reduced ferredoxin via the FNR protein complex. No significant absorbance changes occur in any of the measurments in the case of the grana margins.

markably, neither the grana margins nor the grana core produced any absorbance changes in the reaction mixture, even when they were provided with ascorbate and DCIP as an electron source (Fig. 8). Note, however, the ability of the stroma lamellae to reduce ferredoxin, even in the absence of any artificial electron donors (Fig. 8).

We explored these findings in slightly more detail, by reexamining the three PS-I-rich membrane fractions, whole thylakoids, stroma lamellae, and the grana margins, this time measuring in the split beam mode (Fig. 9). In the upper left-hand portion of Fig. 9 are shown three absorbance traces representing from left to right the kinetics of ferredoxin reduction by thylakoid membranes alone, when supplemented with ascorbate and DCIP, and in the

Table 4
A summary of the rates of electron transport through PS I when either ferrodoxin or $NADP^+$ was the terminal electron acceptor

Membrane fraction	Ferredoxin		$NADP^+$		
	PS II → PS I	Asc/DCIP → PS I	PS II → PS I	Asc/DCIP → PS I	Asc/DCIP → PS I [a]
Thylakoids	77	90	316	318	318
Stroma lamellae	25	190	21	55	290
Grana margins	5	14	0	0	74
Grana core	0	0	0	0	17

The values (μmol/mg Chl per h) measured for both whole chain and partial electron transport are included. The reduction of $NADP^+$ is measured in the presence of 2 μM ferrodoxin.

[a] With added soluble Fd-NAPD reductase, 0.25 units.

presence of $NADP^+$. The rate of ferredoxin reduction for each trace, calculated from a tangent to the initial slope, is shown in Table 4. For unfragmented thylakoids, the rate of ferredoxin reduction catalyzed by whole chain electron transport is about the same as when PS I is supplied with electrons from an artificial source, ascorbate and DCIP. $NADP^+$ completely inhibits the steady state accumulation of reduced ferredoxin, only a slight burst of reduced ferredoxin is observed followed by a new equilibrium state where the reduction and oxidation of ferredoxin occur at equal rates (upper left, $NADP^+$ Fig. 9). At even higher concentrations of $NADP^+$, absolutely no light-induced absorbance change occurs and a straight line is obtained (data not shown). We attribute this effect to the native, membrane-bound ferredoxin:NADP oxidoreductase (FNR) (see western blotting analysis below).

A similar study was carried out for the stromal lamellae (upper right, Fig. 9). We were surprised to find that the stroma lamellae were quite capable of reducing ferredoxin in the absence of any added electron donors (control, Fig. 9), although the rate appears to be much lower than when ascorbate and DCIP are added (Table 4). That we were actually observing whole chain electron transport in the stroma lamellae fraction is confirmed by the inhibition of the light induced absorbance change by DCMU (Fig. 9). DBMIB and KCN also inhibited the reduction of ferredoxin by the stroma lamellae (data not shown). Following the addition of DCMU, the reduction of ferredoxin could be reinstated by adding ascorbate and DCIP to the cuvette (upper right of Fig. 9, lower left trace). Following the measurement with ascorbate and DCIP, $NADP^+$ was added to the cuvette and, as for unfragmented thylakoids, inhibited the steady-state absorbance decrease measured when reduced ferredoxin accumulates in the cuvette.

Again, very little reduction of ferredoxin was observed in the case of the grana margins (lower left Fig. 9). Only a very small change occurs with the addition of ascorbate and DCIP, but certainly not of the magnitude expected based on the PS I content of this fraction (see Table 1). However, $NADP^+$ did prevent even this small change from occurring (lower left Fig. 9), indicating that bound FNR is functioning even in the grana margins.

Even less ferredoxin reduction occurred in the case of the grana core (Table 4), where the inside-out orientation of the vesicles is also expected to hamper access of ferredoxin to the reducing side of PS I.

The inability of the PS I in the grana margins to reduce ferredoxin alone did not prevent them from catalyzing the reduction of $NADP^+$ (Fig. 10). In fact, all of the membrane fractions could reduce $NADP^+$ (Fig. 10). In all cases, the reduction of $NADP^+$ required the addition of ferredoxin. Whole thylakoids produced the highest rates and supplementation with neither ascorbate and DCIP nor with extra FNR improved the rate. Clearly, the amount of catalytically active FNR which remains bound to the membrane of class II thylakoids is saturating, but sonication of the thylakoids may dislodge a great deal of the loosly bound FNR, since the stroma lamellae, grana margins, and

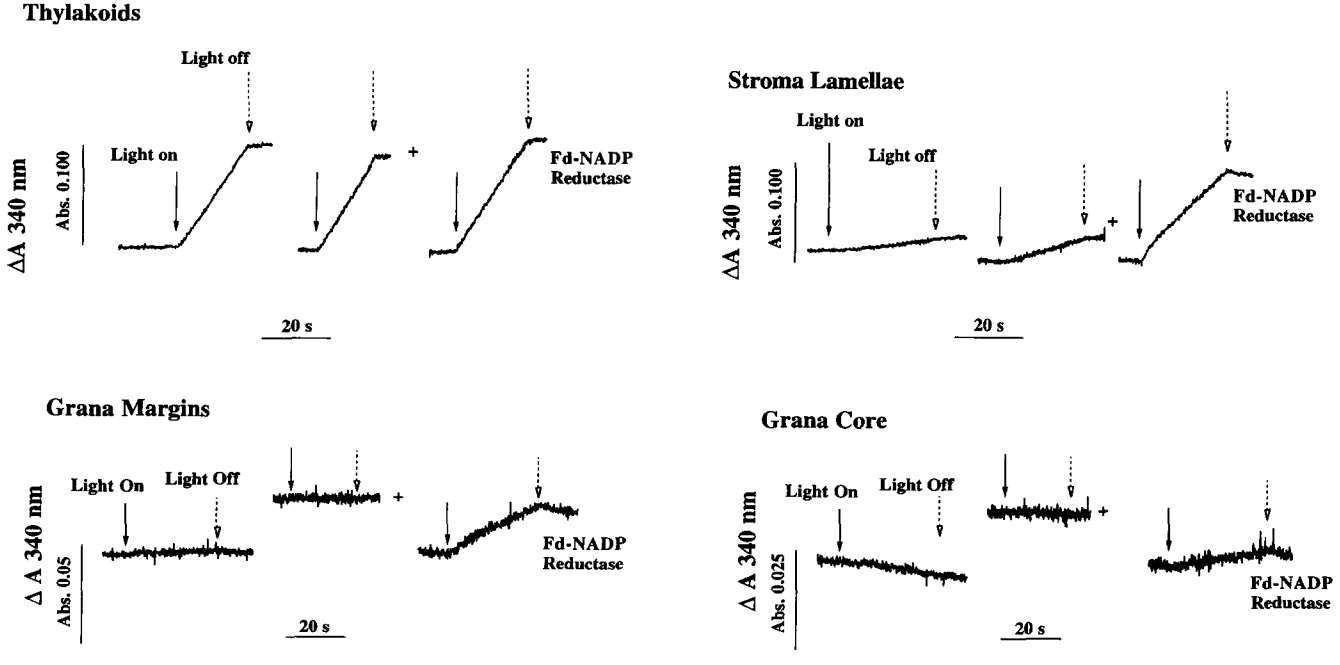

Fig. 10. The reduction of $NADP^+$ by the thylakoid membrane fractions measured as the absorbance decrease at 340 nm. Each sample is measured a total of three times in sequence (the absorbance traces from left to right) first in the absence of any artificial electron donors, following the addition of ascorbate and DCIP(+), and lastly following the addition of extra FNR. In all cases, no reduction occurred in the absence of added ferredoxin (data not shown).

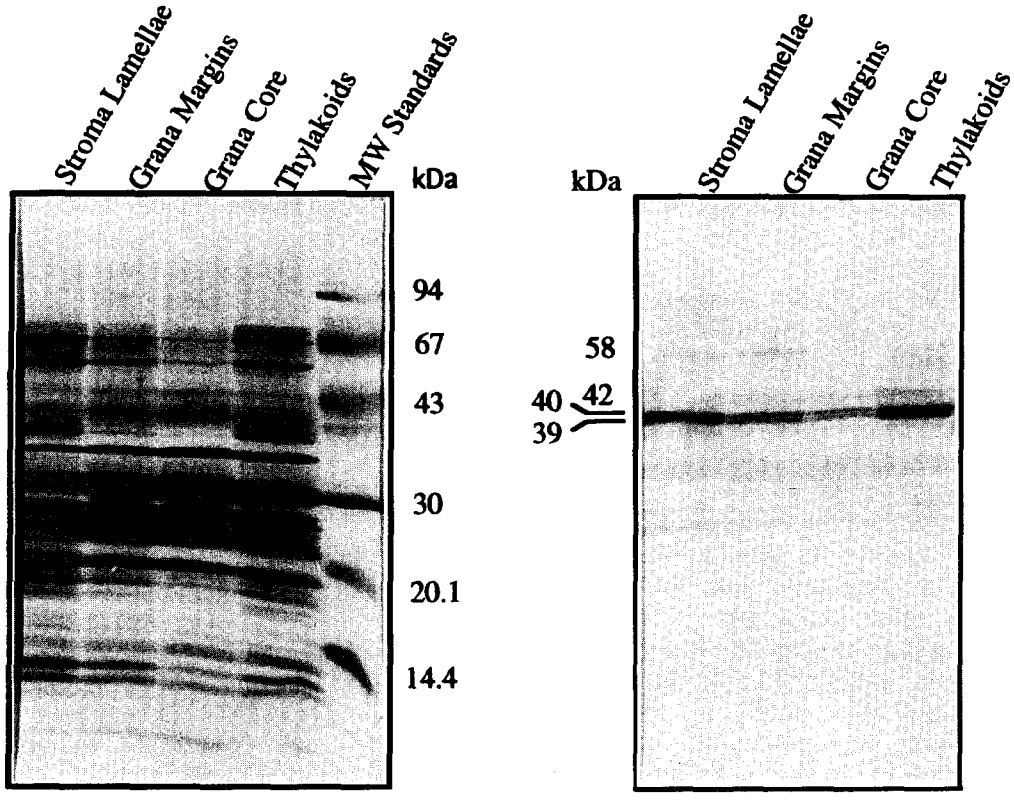

Fig. 11. A western blotting analysis of ferredoxin:$NADP^+$ oxidoreductase for the four types of thylakoid membrane. To the left is shown the Coomassie staining of the total protein, and to the right the bands reacting with the FNR antibody.

grana core all required the addition of extra FNR as well as ascorbate and DCIP to achieve maximum rates (Fig. 10 and Table 4). That portion of FNR which survives the sonication and remains firmly bound to the membrane does not appear to be very active with respect to the reduction of $NADP^+$. Following the addition of ascorbate, DCIP and extra FNR the rate of $NADP^+$ reduction by the stroma lamellae approaches that measured for whole thylakoids (Fig. 10, Table 4). The grana margins also reduce $NADP^+$ at a very satisfactory rate when the reaction mixture is supplied with the necesary components: an electron source and FNR (Fig. 10 and Table 4). Even the grana core vesicles, despite their sidedness, are able to reduce some $NADP^+$ (Fig. 10).

3.7. Western blotting for ferredoxin-NADP reductase

The existence of endogenous, membrane-bound FNR in each of the sub-thylakoid fractions was demonstrated directly by western blotting analysis (Fig. 11). Two closely migrating bands at 40 and 39 kDa and enriched in the stroma lamellae reacted strongly with the FNR antibody (Fig. 11). A significant amount of FNR is also present in the grana margins (40 and 39 kDa) as well as an additional, unidentified band of apparent molecular mass 58 kDa, whose reaction with anti-FNR is strongest in the grana margins.

4. Discussion

This study complements our initial report describing the isolation and characterization of the chloroplast grana margins [1] and provides new information regarding the unique nature of this area of the thylakoid membrane continuum.

The sonication and separation method we have employed here was developed subsequent to the first report to provide for a greater yield of the margin vesicles. We routinely obtain between 600 and 1000 μg Chl margins from 20 mg Chl thylakoids. We use centrifugation to speed up the partitioning process, cutting down the time required to complete the isolation, which runs about 4 to 5 h starting with whole spinach leaves. Since we find that sonication of the inside-out grana vesicles (B4) generates two types of vesicle, one large and enriched for PS II, and another, much smaller which is enriched for PS I (Fig. 3 and see Table 1), it is possible that a combination of sonication and differential centrifugation might also provide a satisfactory method for preparation of the core and margins of the grana.

In terms of the total pigment-protein composition, the grana margins possess biochemical features of both the appressed and non-appressed membrane domains (Table 1, Fig. 4 and Fig. 5 and [1]). We obtain about the same levels of PS II and PS I (KCN-treated fractions) electron transport for the grana margins as for whole thylakoids (Table 2).

There is about 1.7-times more chlorophyll *b* per total chlorophyll in the grana margins than in the stroma lamellae (Table 1). However, neither the light saturation kinetics of PS II activity presented here (Fig. 7, Table 2) nor the kinetics of fluorescence induction published earlier [1] have been able to demonstrate that this extra chlorophyll *b* in the grana margins is functionally coupled to PS II. On the contrary, our data and those of others [6,32] support the notion that the majority of the chlorophyll *b* in the grana margins is associated with PS I (compare K_M values among fractions for PS II and PS I in Table 2 and see [1,32], where photo-oxidation kinetics of P700 was used to study PS I antenna size). Albertsson et al. have shown, after analyzing several membrane fractions from the outer, middle, and innermost areas of the granal disc, that the PS II with the largest antennae lie closest to the core of the grana, while the PS II with the smallest antennae are located farthest away in the grana margins [42,43]. The combined evidence indicates, therefore, that the PS II centers located in the grana margins are, at least with respect to antenna size, of the PS II_β sub-type.

However, with regard to reducing potential, the PS II centers in the grana margins are more like the PS II in the grana core (Table 3). Therefore, we suggest that the grana margins contain predominantly Q_B reducing PS II_β whereas the stroma lamellae contain primarily non-Q_B reducing PS II_β [39]. The margins of the grana is the only sub-thylakoid membrane region studied thus far which contains mainly PS II_β and PS I_α. Furthermore, these results support a model of the thylakoid membrane where the inactive and active PS II_β centers are located in different regions of the thylakoid.

The PS I centers located in the grana margins and core membrane fractions were unable to reduce ferredoxin, even in the presence of ascorbate and DCIP, whereas the PS I in the stroma lamellae reduced ferredoxin even in the absence of any artificial electron donors, showing that the PS II_β centers in the stroma lamellae are capable of reducing the PQ pool to some extent and therefore are also capable of supplying or 'poising' PS I with electrons (Figs. 9 and 10, Table 4) [31].

The grana margins were, however, able to reduce $NADP^+$ when supplied with the necessary components (ferredoxin, FNR, ascorbate and DCIP), as were all other membrane fractions examined (Fig. 10). No whole-chain electron transport was found due to the absence of plastocyanin. The rates of $NADP^+$ reduction, a two-electron process, observed for the right-side-out membrane fractions, i.e., thylakoids, the stroma lamellae, and the grana margins (Table 4), are roughly one-half the corresponding V_{max} values for PS I electron transport, a one-electron process when Methyl viologen is the acceptor (Table 2, control). The PS I centers in the grana margins are, apparently, able to reduce ferredoxin only in the presence of $NADP^+$ (i.e., when $NADP^+$ is concurrently reduced), whereas the PS I in the stroma lamellae can reduce ferredoxin independent of $NADP^+$ reduction. This may reflect a difference in function between the granal and stroma lamellae PS I populations, with the former primarily involved in non-cyclic electron transport. Several C3 sun and shade plant species have very similar quantum yields (0.11 mol O_2/mol photons) [44]. The argument has been made that this constancy among plant species, irrespective of the light intensity during growth, implies, among other things, that the number of PS I centers participating in cyclic electron transport must be controlled [16]. Furthermore, analysis of electron microscopic images of thin sections from chloroplasts of different plant species shows that about 80% of the membrane belongs to the grana area and 20% to the stroma lamellae. Assuming that the chlorophyll is uniformly distributed over the entire thylakoid membrane and that only the light quanta striking the grana are effectively utilized for linear electron transport (O_2 evolution), the quantum yield calculated for the thylakoid as a whole is 0.1 (Albertsson, P.-Å., unpublished data), about the same as the experimentally determined values reported in [44].

It is known that, upon binding ferredoxin, FNR forms transitory complexes with PS I in the thylakoid membrane [45]. It is also known that detergent isolated particles of PS I contain FNR [46]. In this regard,it is intriguing that the western blotting analysis of FNR demonstrated the presence of an extra band enriched in the grana margins (Fig. 11). It is possible that associations of this type between multi-subunit protein complexes are one way to direct reducing equivalents to either ferredoxin or $NADP^+$. It would be interesting to know how the phosphorylation of FNR during high light conditions may influence these types of association [47].

Although the explanation and significance underlying the inability of the PS I in the grana margins to reduce ferredoxin in the absence of $NADP^+$ is not certain, these results show absolutely that this membrane fraction is unique and not the same as the stroma lamellae fraction. The PS I centers located in the fraction we call the grana margins must derive from the same inside-out membrane domain as does the grana core fraction, since we find that neither contains any plastocyanin based on the results of the experiments with KCN (Fig. 6a and 6b, Table 2). Furthermore, these PS I centers must be closely associated with the PS II of the appressed area if they are to be captured on the same membrane sheet during the formation of the inside-out vesicle when whole thylakoids are sonicated. Since western blotting analysis shows that FNR exists in the grana margins, it can be argued that all the

components necessary to carry out linear electron transport are represented within the confines of the grana compartment.

Acknowledgements

We thank Birger-Lindberg Møller for the gift of the ferredoxin:$NADP^+$ oxidoreductase antibodies and Ingun Sundén and Agneta Persson for technical assistance. This work was supported by the Swedish Natural Sciences Research Council.

References

[1] Wollenberger, L., Stefansson, H., Yu, S.-G. and Albertsson, P.-Å. (1994) Biochim. Biophys. Acta 1184, 93–102.
[2] Albertsson, P.-Å. (1986) Partition of Cell Particles and Macromolecules, 3rd Edn., Wiley, New York.
[3] Walter, H., Brooks, D.E. and Fisher, D. (eds.) (1985) Partitioning in Aqueous Two-Phase Systems, Academic Press, New York.
[4] Walter, H. and Johansson, G. (eds.) (1994) Aqueous Two-Phase Systems. Methods Enzymol. Vol. 228.
[5] Svensson, P. and Albertsson, P.-Å. (1989) Photosynth. Res. 20, 249–259.
[6] Andreasson, E. and Albertsson, P.-Å. (1992) Biochim. Biophys. Acta 1141, 175–182.
[7] Vaughn, K.C., Vierling, E., Duke, S.O. and Alberte, R.S. (1983) Plant Physiol. 73, 203–207.
[8] Webber, A.N., Platt-Aloia, K.A., Heath, R.L. and Thomson, W.W. (1988) Physiol. Plant. 72, 288–297.
[9] Allred, D.R. and Staehelin, L.A. (1985) Plant Physiol. 78, 194–202.
[10] Vallon, O., Wollman, F.A. and Olive, J. (1986) Photobiochem. Photobiophys. 12, 203–220.
[11] Jacobi, G. and Lehmann, H. (1968) Z. Pflanzen. Physiol. 59, 457–476.
[12] Sane, P.V., Goodchild, D.J. and Park, R.B. (1970) Biochim. Biophys. Acta 216, 162–178.
[13] Arntzen, C.J., Dilley, R.A., Peters, G.A. and Shaw, E.R. (1972) Biochim. Biophys. Acta 256, 85–107.
[14] Albertsson, P.-Å., Andreasson, E. and Svensson, P. (1990) FEBS Lett. 273, 36–40.
[15] Anderson, J.M. (1989) Physiol. Plant. 76, 243–248.
[16] Anderson, J.M. and Thomson, W.W. (1989) Dynamic molecular organization of the plant thylakoid membrane. In Towards an Understanding of Photosynthesis, Multiple Approaches to a Common Goal (Briggs, W., ed.), pp. 161–182. Alan R. Liss, New York.
[17] Albertsson, P.-Å., Andreasson, E., Stefansson, H. and Wollenberger, L. (1994) Methods Enzymol. 228, 469–482.
[18] Yu, S.-G., Björn, G. and Albertsson, P.-Å. (1993) Photosynth. Res. 37, 227–236.
[19] Andreasson, E., Svensson, P., Weibull, C. and Albertsson, P.-Å. (1988) Biochim. Biophys. Acta 936, 339–350.
[20] Beardon Jr, J.C. (1978) Biochim. Biophys. Acta 533, 525–529.
[21] Kjellbom, P. and Larsson, C. (1984) Physiol. Plant. 62, 501–509.
[22] Melis, A. and Brown, J.S. (1980) Proc. Natl. Acad. Sci. USA 77, 4712–4716.
[23] Arnon, D.I. (1949) Plant Physiol. 24, 1–15.
[24] Lichtenthaler, H.K. (1987) Methods Enzymol. 148, 350–382.
[25] Cleland, R.E. and Bendall, D.S. (1992) Photosynth. Res. 34, 409–418.
[26] Fasman, G.D. (ed.) (1976) Handbook of Biochemistry and Molecular Biology, 3rd Edn., Physical and Chemical Data, Volume II, CRC Press, Cleveland.
[27] Laemmli, U.K. (1970) Nature 227, 680–685.
[28] Juhler, R.K., Andreasson, E., Yu, S.-G. and Albertsson, P.-Å. (1993) Photosynth. Res. 35, 171–178.
[29] Bassi, R., Pineau, B., Dainese, P. and Marquardt, J. (1993) Eur. J. Biochem. 212, 297–303.
[30] Rijgersberg, C.P., Amesz, J., Thielen, A.P.G.M. and Swager, J.A. (1979) Biochim. Biophys. Acta 545, 473–482.
[31] Anderson, J.M. and Melis, A. (1983) Proc. Natl. Acad. Sci. USA 80, 745–749.
[32] Svensson, P., Andreasson, E. and Albertsson, P.-Å. (1991) Biochim. Biophys. Acta 1060, 45–50.
[33] Hofstee, B.H.J. (1952) Science 116, 329–331.
[34] Hofstee, B.H.J. (1959) Nature Lond. 184, 1296–1298.
[35] Haehnel, W., Berzborn, R.J. and Andersson, B. (1981) Biochim. Biophys. Acta 637, 389–399.
[36] Melis, A. (1978) FEBS Lett. 95, 202–206.
[37] Horton, P. (1981) Biochim. Biophys. Acta 635, 105–110.
[38] Thielen, A.P.G.M. and Van Gorkom, H.J. (1981) FEBS Lett. 129, 205–209.
[39] Henrysson, T. and Sundby, C. (1990) Photosynth. Res. 25, 107–117.
[40] Petrouleas, V. and Diner, B.A. (1987) Biochim. Biophys. Acta 893, 126–137.
[41] Govindjee. (1990) Photosynth. Res. 25, 151–160.
[42] Albertsson, P.-Å. and Yu, S.-G. (1988) Biochim. Biophys. Acta 936, 215–221.
[43] Albertsson, P.-Å., Yu, S.-G. and Larsson, U.K. (1990) Biochim. Biophys. Acta 1016, 137–140.
[44] Björkman, O. and Demmig, B. (1987) Planta 170, 489–504.
[45] Wagner, R., Carrillo, N., Junge, W. and Vallejos, R.H. (1982) Biochim. Biophys. Acta 680, 317–331.
[46] Andersen, B., Scheller, H.V. and Møller, B.L. (1992) FEBS Lett. 311, 169–173.
[47] Hodges, M., Miginiac-Maslow, M., Marechal, P.L. and Remy, R. (1990) Biochim. Biophys. Acta 1052, 446–452.